Disorder and Suppression of Quantum Confinement Effects in Pd Nanoparticles

J. G. Hou,[1,*] Bing Wang,[1] Jinlong Yang,[1,†] Kedong Wang,[1] Wei Lu,[1] Zhenyu Li,[1] Haiqian Wang,[1] D. M. Chen,[1,2] and Qingshi Zhu[1]

[1]*Structure Research Laboratory and Laboratory of Bond Selective Chemistry, University of Science and Technology of China, Hefei, Anhui 230026, People's Republic of China*

[2]*Rowland Institute at Harvard, Harvard University, Cambridge, Massachusetts 02142, USA*

(Received 11 November 2002; published 19 June 2003)

Size-selectable ligand-passivated crystalline and amorphous Pd nanoparticles (< 4 nm) are synthesized by a novel two-phase process and verified by high-resolution transmission electron microscopy. Scanning tunneling spectroscopy preformed at 5 K on these two types of nanoparticles exhibits clear Coulomb blockade and Coulomb staircases. Size dependent multipeak spectral features in the differential conductance curve are observed for the crystalline Pd particles but not for the amorphous particles. Theoretical analysis shows that these spectral features are related to the quantized electronic states in the crystalline Pd particle. The suppression of the quantum confinement effect in the amorphous particle arises from the reduction of the degeneracy of the eigenstates and the level broadening due to the reduced lifetime of the electronic states.

DOI: 10.1103/PhysRevLett.90.246803 PACS numbers: 73.22.–f, 68.37.Ef, 73.23.Hk

It is a widely accepted view that when the size of a material is reduced to a few nanometers the material properties will be dominated by quantum effects. In the past decade, a number of studies have been focused on the correlations between the properties and the size, shape, and composition of crystalline nanoparticles [1–4]. On the other hand, it is well known that the amorphous solids have distinct transport properties from the crystalline ones [5,6]. What is the fundamental impact of disorder on the properties of nanoscale systems is still an open question. In this Letter, we present a comparative study of thiolstabilized crystalline and amorphous Pd nanoparticles. We show that reducing the size alone is insufficient to push a system into its quantum regime. Disorder extends the semiclassical behavior of metallic particle into a regime that would otherwise be fully quantum mechanical in an ordered system. The degree of the atomic order of a nanoparticle plays an equally important role in determining its quantum or classical nature.

Using the two-phase method [7,8], we were able to controllably synthesize nearly monodispersed Pd nanoparticles, either crystalline or amorphous. Synthesis of crystalline Pd nanoparticles of 2 nm in diameter were modified as follows: Added 460 mg PVP [poly (*N*-vinyl-2-pyrrolidone)] into 50 ml ethanol solution containing 2 mg $PdCl_2$, and then mixed with an equal volume of 2 mM toluene solution of dodecanethiol (DT). After reaction the DT-stabilized palladium nanoparticles were separated and purified, and then redissolved into toluene. The amorphous Pd nanoparticles were synthesized by modifying the above pathway in two aspects: (i) the ethanol solution was replaced by the hydrochloric acid solution, and (ii) 3 mg $NaBH_4$ was added into the 50 ml water forming the initial mixture. For either case, the size of the thiolstabilized Pd nanoparticles can be controlled by adjusting the concentration of $PdCl_2$ in the solution and the temperature during the reflux.

Chemically synthesized Pd nanoparticles were structurally characterized by a JOEL 2100 high-resolution electron microscope (HREM). The HREM analysis shows that our synthesized thiolstabilized Pd nanoparticles are nearly monodispersed and the core size ranges from 1.5 to 4 nm in diameter (insets to Fig. 1). The typical electron diffraction patterns and HREM images of Pd nanoparticles in Fig. 1 show distinct atomic structures between crystalline Pd (*c*-Pd) and amorphous Pd (*a*-Pd) nanoparticles. The regular lattice pattern can be resolved for the *c*-Pd nanoparticles, but not for the *a*-Pd nanoparticles.

With a scanning tunneling microscope (STM) set up, we measured the single electron tunneling (SET) spectra of these two types of Pd nanoparticles. SET has been proven to be a unique technique for the study of electronic structure of individual nanoparticles [1,3,4,9–11]. In our experiment, a drop of diluted toluene solution of *c*-Pd or *a*-Pd particles was spread on a piece of Au (111) single crystal substrate. After a slow evaporation of the solvent, the sample was transferred into the vacuum chamber of the STM (Omicron) operated at 5 K, where STM and scanning tunneling spectroscopy (STS) were performed. STM images show that the thiolstabilized Pd nanoparticles on the Au surface are well separated from each other [lower inset of Fig. 2(a)]. SET spectra were measured in a double barrier tunneling junction (DBTJ) formed by positioning the Pt/Ir tip above the nanoparticle [upper inset to Fig. 2(a)]. Two typical *I*-*V* curves for the *c*-Pd (curve 1) and *a*-Pd (curve 2) particles of about 2 nm in diameter are shown in Fig. 2(a). Both curves present clear equidistant steps of Coulomb blockade (CB) and Coulomb staircases due to the same mechanism of single

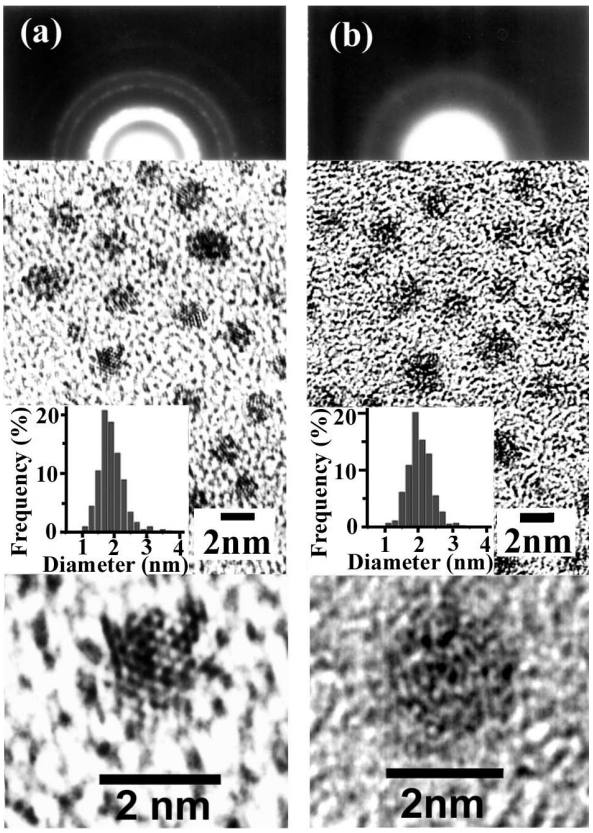

FIG. 1. Electron diffraction patterns and HREM images of Pd nanoparticles with an average size of 2 nm: (a) *c*-Pd nanoparticles, and (b) *a*-Pd nanoparticles. The insets are the histogram of the size distributions.

electron charging effect as shown by the fitted result (curve 3) [11], but some additional fine structures also appear in the *I-V* curve 1 for the *c*-Pd particle.

While the main current steps are similar, the fine structures are quite different between the spectra of the *c*-Pd and *a*-Pd particles. Figure 2(b) shows three pairs of numerical differential conductance spectra of Pd nanoparticles with various sizes. The data for each pair were obtained from separate measurements of the *c*-Pd and *a*-Pd particles with roughly equal size. In sharp contrast to the rich multipeak features of the *c*-Pd particles, only equally spaced Coulomb charging peaks are observed for the *a*-Pd particles.

The difference in the fine features of the *I-V* spectra is independent of the measurement conditions. For example, when the junction capacitance C_2 is varied by adjusting the tip-particle separation, the features of the Coulomb charging peaks do not change for either type of Pd particles [see Fig. 3(a)]. In order to exclude any possible spurious effect of the tip, we mixed two types of Pd particles in one sample and used the same tip to image and collect *I-V* spectra for either type of Pd particles. As an example, we show an STM image of two particles labeled as *A* and *B* in Fig. 3(b), and their typical STS

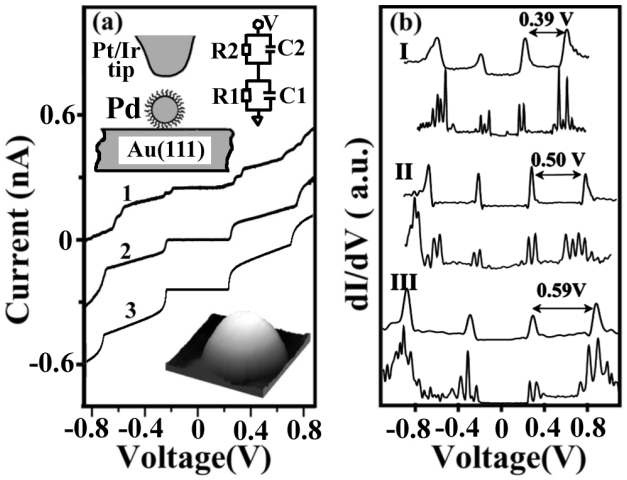

FIG. 2. (a) Curves 1 and 2 are typical *I-V* curves for a *c*-Pd and an *a*-Pd particle of about 2 nm in diameter with the set point parameters being (1.8 V, 1.0 nA), respectively. Curve 3 is a fitting curve using the orthodox theory by assuming the DOS is a constant (fitting parameters: $C_1 = 0.32$ aF, $C_2 = 0.34$ aF, $R_1 = 40$ MΩ, $R_2 = 2.1$ GΩ, and $Q_0 = -0.006e$). The top inset is a schematic of the STM double tunnel junction. The bottom inset is a 6×6 nm STM image, showing a Pd nanoparticle. (b) Three pairs of numerical differential conductance spectra of Pd nanoparticles with various sizes of 2.5, 2.0, and 1.6 nm, respectively. In each pair of curves I, II, and III, the lower one is for a *c*-Pd particle, and the upper one for an *a*-Pd particle. The spectra were offset along the *V* axis to center the Coulomb gaps at zero bias.

spectra in Fig. 3(c). The STS spectra of *A* and *B* particles have the same spectral features as those presented in Fig. 2 for *c*-Pd and *a*-Pd particles, respectively. Thus, the different features in STS spectra are not caused by the tip effect.

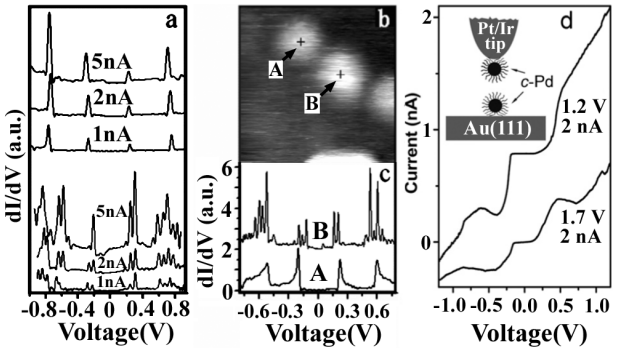

FIG. 3. (a) The numerical differential conductance spectra of two 2 nm *a*-Pd and *c*-Pd particles with various set point of the tunneling currents. (b) A STM image showing an *a*-Pd particle *A* and a *c*-Pd particle *B*; (c) *dI/dV* spectra acquired on particle *A* and particle *B*, respectively. (d) *I-V* curves measured on two coupled *c*-Pd particles with the structure depicted as inset. The zero current gaps of curves were centered at zero bias for comparison.

To ensure that the rich spectral structures obtained for c-Pd particles are not caused by the fluctuating background charge (Q_0 noise) [12,13], but related to their electronic structures, we performed a STS measurement on a structure of two coupled c-Pd particles formed by the STM manipulation [14]. The negative differential resistance (NDR) effect is observed in the I-V curves [Fig. 3(d)]. Clearly, the Q_0 noise cannot result in NDR, and the origin of NDR should be the resonance tunneling between the discrete energy levels of two coupled c-Pd nanoparticles. We did not observe the NDR effect for the coupled a-Pd particles. Thus, we can conclude that the presence/absence of the fine features in the I-V spectra is related to the intrinsic electronic properties of c-Pd and a-Pd particles.

When the central island of an SET is very small, the SET spectra reflect the interplay between the discrete energy level due to quantum confinement and the CB effect [15]. The CB effect gives equidistant main current steps in the I-V curves, while the discrete energy levels cause additional nonequidistant current steps [1,3,4,9–11]. The multilevel processes have been invoked to explain the complex SET spectra on Au [9,10] and semiconductor nanoparticles [3,4]. Our results for the c-Pd particles reveal that metallic nanoparticles can also give rise to peaks resembling the "shell structure" of the semiconductor nanoparticles [3,4], and we attribute them to the same quantum confinement effect. The fact that there is no fine structure in the SET spectra of the a-Pd particles, therefore, implies that the effect of discrete energy levels is strongly suppressed. This cannot be caused by the effects from the surface boundary only, otherwise we can expect both c-Pd and a-Pd particles would give rise to similar electron energy spectra. It is thus clear that, in addition to the size, order and disorder also play a critical role in determining a system's quantum or classical nature.

To gain a more detailed understanding on the role of order vs disorder in a particle, we should consider the electronic structures of Pd particles. We used the tight-binding (TB) method, with the TB parameters taken from Ref. [16], to calculate the electronic structures of naked c-Pd and a-Pd nanoparticles. As an example, we show the geometric and electronic structures for the 2.2 nm c-Pd and a-Pd particles in Fig. 4. In the c-Pd particle some levels have high degrees of degeneracy [Fig. 4(a), inset], resulting in the average energy spacing of levels in the c-Pd particle is about 3 times larger than that in the a-Pd particle [Fig. 4(b) inset]. Applying these discrete energy spectra directly to the orthodox theory in which the temperature dependent Fermi distributions of the electrodes and the particle were taken into account in the golden rule [17], we then calculated the dI/dV-V curves. For the c-Pd particle, our calculated dI/dV-V curve [Fig. 4(a)] reproduces qualitatively the observed SET spectrum, but to explain quantitatively our measured

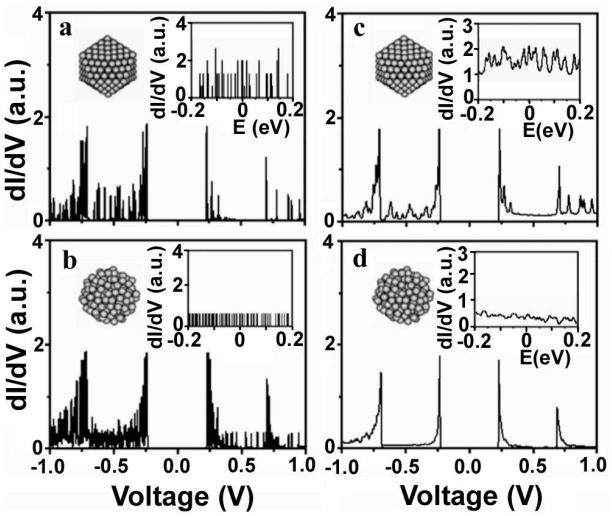

FIG. 4. Calculated SET spectra of 2.2 nm c-Pd and a-Pd particles obtained by the orthodox theory with different electronic structures: (a) c-Pd particle with discrete energy levels, (b) a-Pd particle with discrete energy levels, (c) c-Pd particle with Lorentzian extended discrete energy levels of line width broadening of 4.3 meV due to dynamic effect, (d) a-Pd particle with Lorentzian extended discrete energy levels of line width broadening of 4.3 meV due to dynamic effect. Insets show the atomic and electronic structures accordingly. The junction parameters used for the spectra are $C_1 = 0.32$ aF, $C_2 = 0.34$ aF, $R_1 = 40$ MΩ, $R_2 = 2.1$ GΩ, and $Q_0 = -0.006e$).

SET spectra, one may need to consider the ligand and nonequilibrium many-body effects [18]. For a-Pd particles, theoretical results still show additional peaks between the Coulomb charging peaks [see Fig. 4(b)], which should be observable within the resolution of our STM. But these peaks are clearly absent in our observation. For our controlled calculation of the I-V (and dI/dV) curves, our apparatus limitation of 2 mV is represented by a Gaussian function which is convoluted with the I-V spectra. The results show that the apparatus limitation do not suppress the fine structures in calculated dI/dV curves both for crystalline and amorphous Pd particles. Thus, the differences between the static atomic/electronic structures of nanoparticles alone cannot explain our experimental results, and the dynamic effects would have to be taken into consideration here.

In nanoparticles, the e-e scattering is enhanced due to surface induced reduction of the Coulomb interaction screening by conduction and core electrons, and plays a key role in their transport properties at low temperature [19,20]. We estimate the effective scattering lifetime $\tau_{e\text{-}e}$ due to e-e interaction of a 2.2 nm a-Pd particle to be 195 fs using the measured $\tau_{e\text{-}e}$ of low-lying states of small Pd clusters [21] and an approximate relationship $\tau_{e\text{-}e} \propto N^{1/3}$ (N is the number of atoms in cluster) which holds for a small variation of $N^{1/3}$ [19]. With the Heisenberg energy-time uncertainty principle, we obtain the level broadening from the $\tau_{e\text{-}e}$ to be 3.3 meV.

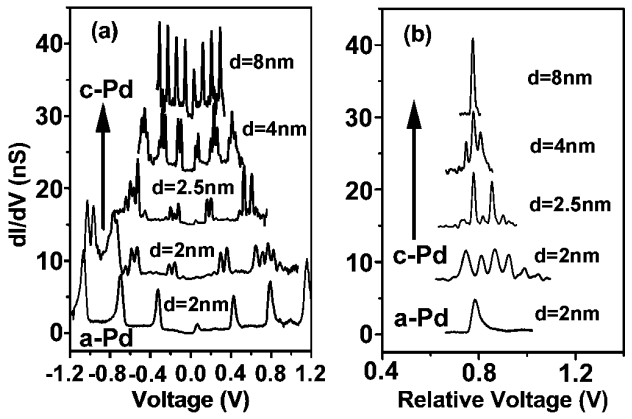

FIG. 5. (a) dI/dV spectra of c-Pd particles and an a-Pd particle. For clarity, curves are shifted vertically. (b) Comparison of fine spectral features of the second CB steps for various particle size. Peaks are shifted in voltage coordinate.

Besides the e-e scattering, the electron-phonon (e-p) scattering also contributes the electron relaxation dynamics [18]. At low temperature, the probability of phonon adsorption is negligible, and only emission may take place. The e-p scattering lifetime $\tau_{e\text{-}p}$ decreases with the increase of the size of nanoparticle since there are more vibrational degrees of freedom in a larger nanoparticle. We can get the upper limit of the $\tau_{e\text{-}p}$ of our nanoparticles from the measured $\tau_{e\text{-}p}$ of small Pd clusters [21] to be 700 fs. This $\tau_{e\text{-}p}$ contributes the additional level broadening about 1 meV. Thus, the total level broadening is at least 4.3 meV due to the dynamic effect.

Using the estimated level broadening parameter, we obtained the densities of states (DOS) of the c-Pd and a-Pd particle by a Lorentzian extension of the discrete energy levels and a summation over them. Applying these DOS's to the orthodox theory, we obtained the new theoretical dI/dV-V curves of the c-Pd and a-Pd particle, respectively, shown in Figs. 4(c) and 4(d). In Fig. 4(c), the additional peaks between the Coulomb peaks in the spectrum of c-Pd particle still persist, while all additional peaks between the Coulomb charging peaks disappear in the spectrum of a-Pd particle, in good agreement with our experiments. Thus, both the static and dynamic electronic effects in an a-Pd particle result in its SET spectrum being dominated by the pure charging effect. So, the quantum effects associated with the quantized states is suppressed significantly in an a-Pd particle with a size as small as about 2 nm.

Thus in general, both the particle size and its internal order play equally important roles in determining whether such a particle will exhibit quantum properties. For c-Pd particles, it is evident from Fig. 5 (top four curves) that there is an increasing complexity in the spectra features as the particle size reduces. For an a-Pd particle of the comparable sizes, however, the discrete energy level effect is completely suppressed. It is interesting to see in Fig. 5(b) that the shape of the SET peak of a 2 nm a-Pd particle appear to be closer to that of a c-Pd particle that is 4 times larger (8 nm in diameter). Moreover, one can see that the peak width increases with deceasing particle size. This is consistent with the dynamic effects discussed above. With the decrease of the size of nanoparticle, the enhanced e-e scattering will result in the larger level broadening.

We thank Professor Takashi Nagata for his stimulating discussions and help in the preparation of samples. This work was supported by the National Project for the Development of Key Fundamental Sciences in China (No. G1999075305, No. G2001CB3095), and by the National Natural Science Foundation of China.

*Corresponding author.
Email address: jghou@ustc.edu.cn
†Corresponding author.
Email address: jlyang@ustc.edu.cn

[1] For a review, see J. von Delft and D. C. Ralph, Phys. Rep. **345**, 61 (2001).
[2] D. M. Mittleman *et al.*, Phys. Rev. B **49**, 14 435 (1994).
[3] U. Banin, Y.W. Cao, D. Katz, and O. Millo, Nature (London) **400**, 542 (1999).
[4] O. Millo, D. Katz, Y.W. Cao, and U. Banin, Phys. Rev. Lett. **86**, 5751 (2001).
[5] P.W. Anderson, Phys. Rev. **109**, 1492 (1958).
[6] A. Miller and E. Abrahams, Phys. Rev. **120**, 745 (1960).
[7] M. Brust, M. Walker, D. Bethell, D. J. Schiffrin, and R. Whyman, J. Chem. Soc. Chem. Commun., 801 (1994).
[8] N. Toshima, T. Yonezawa, and K. Kushihashi, J. Chem. Soc. Faraday Trans. **89**, 2537 (1993).
[9] D. C. Ralph, C. T. Black, and M. Tinkham, Phys. Rev. Lett. **74**, 3241 (1995).
[10] D. Davidović and M. Tinkham, Phys. Rev. Lett. **83**, 1644 (1999), and references therein.
[11] B. Wang *et al.*, Phys. Rev. B **63**, 035403 (2001).
[12] J. G. A. Dubois, E. N. G. Verheijen, J.W. Gerritsen, and H. van Kempen, Phys. Rev. B **48**, 11260 (1993).
[13] N. M. Zimmerman, J. L. Cobb, and A. F. Clark, Phys. Rev. B **56**, 7675 (1997).
[14] C. G. Zeng *et al.*, Appl. Phys. Lett. **77**, 3595 (2000).
[15] D.V. Averin, A. N. Korotkov, and K. K. Likharev, Phys. Rev. B **44**, 6199 (1991).
[16] M. J. Mehl and D. A. Papaconstantopoulos, Phys. Rev. B **54**, 4519 (1996).
[17] M. Amman, R. Wilkins, E. Ben-Jacob, P. D. Maker, and R. C. Jaklevic, Phys. Rev. B **43**, 1146 (1991).
[18] O. Agam, N. S. Wingreen, B. L. Altshuler, D. C. Ralph, and M. Tinkham, Phys. Rev. Lett. **78**, 1956 (1997).
[19] C. Voisin *et al.*, Phys. Rev. Lett. **85**, 2200 (2000).
[20] U. Sivan, Y. Imry, and A. G. Aronov, Europhys. Lett. **28**, 115 (1994).
[21] N. Pontius, G. Lüttgens, P. S. Bechthold, M. Neeb, and W. Eberhardt, J. Chem. Phys. **115**, 10 479 (2001).